

1 **A GENERALISED RANDOM ENCOUNTER MODEL FOR ESTIMATING**
2 **ANIMAL DENSITY WITH REMOTE SENSOR DATA**

3 **Running title: A generalised random encounter model for animals.**

4 **Word count:** 7647

5 **Authors:**

6 Tim C.D. Lucas^{1,2,3,†}, Elizabeth A. Moorcroft^{1,4,5,†}, Robin Freeman⁵, Marcus J. Rowcliffe⁵,
7 Kate E. Jones^{2,5}

8 **Addresses:**

9 1 CoMPLEX, University College London, Physics Building, Gower Street, Lon-
10 don, WC1E 6BT, UK

11 2 Centre for Biodiversity and Environment Research, Department of Genetics,
12 Evolution and Environment, University College London, Gower Street, London,
13 WC1E 6BT, UK

14 3 Department of Statistical Science, University College London, Gower Street,
15 London, WC1E 6BT, UK

16 4 Department of Computer Science, University College London, Gower Street,
17 London, WC1E 6BT, UK

18 5 Institute of Zoology, Zoological Society of London, Regents Park, London, NW1
19 4RY, UK

20 † First authorship shared.

21 **Corresponding authors:**

22 Kate E. Jones,
23 Centre for Biodiversity and Environment Research,
24 Department of Genetics, Evolution and Environment,
25 University College London,
26 Gower Street,
27 London,
28 WC1E 6BT,

29 UK

30 kate.e.jones@ucl.ac.uk

31

32 Marcus J. Rowcliffe,

33 Institute of Zoology,

34 Zoological Society of London,

35 Regents Park,

36 London,

37 NW1 4RY,

38 UK

39 marcus.rowcliffe@ioz.ac.uk

ABSTRACT

40
41 **1:** Wildlife monitoring technology is advancing rapidly and the use of remote sen-
42 sors such as camera traps and acoustic detectors is becoming common in both the
43 terrestrial and marine environments. Current methods to estimate abundance or
44 density require individual recognition of animals or knowing the distance of the
45 animal from the sensor, which is often difficult. A method without these require-
46 ments, the random encounter model (REM), has been successfully applied to es-
47 timate animal densities from count data generated from camera traps. However,
48 count data from acoustic detectors do not fit the assumptions of the REM due to
49 the directionality of animal signals.

50 **2:** We developed a generalised REM (gREM), to estimate absolute animal density
51 from count data from both camera traps and acoustic detectors. We derived the
52 gREM for different combinations of sensor detection widths and animal signal
53 widths (a measure of directionality). We tested the accuracy and precision of this
54 model using simulations of different combinations of sensor detection widths and
55 animal signal widths, number of captures, and models of animal movement.

56 **3:** We find that the gREM produces accurate estimates of absolute animal density
57 for all combinations of sensor detection widths and animal signal widths. How-
58 ever, larger sensor detection and animal signal widths were found to be more pre-
59 cise. While the model is accurate for all capture efforts tested, the precision of the
60 estimate increases with the number of captures. We found no effect of different
61 animal movement models on the accuracy and precision of the gREM.

62 **4:** We conclude that the gREM provides an effective method to estimate absolute
63 animal densities from remote sensor count data over a range of sensor and animal
64 signal widths. The gREM is applicable for count data obtained in both marine
65 and terrestrial environments, visually or acoustically (e.g., big cats, sharks, birds,
66 echolocating bats and cetaceans). As sensors such as camera traps and acous-
67 tic detectors become more ubiquitous, the gREM will be increasingly useful for
68 monitoring unmarked animal populations across broad spatial, temporal and tax-
69 onomic scales.

Keywords. Acoustic detection, camera traps, marine, population monitoring, simulations, terrestrial

INTRODUCTION

The density of animal populations is one of the fundamental measures in ecology and conservation and has important implications for a range of issues, such as sensitivity to stochastic fluctuations (Wright & Hubbell, 1983) and extinction risk (Purvis *et al.*, 2000). Monitoring animal population changes in response to anthropogenic pressure is becoming increasingly important as humans rapidly modify habitats and change climates (Everatt *et al.*, 2014). Sensor technology, such as camera traps (Karanth, 1995; Rowcliffe & Carbone, 2008) and acoustic detectors (Acevedo & Villanueva-Rivera, 2006; Walters *et al.*, 2012) are widely used to monitor changes in animal populations as they are efficient, relatively cheap and non-invasive, allowing for surveys over large areas and long periods (Rowcliffe & Carbone, 2008; Kessel *et al.*, 2014; Walters *et al.*, 2013). However, converting sampled count data into estimates of density is problematic as detectability of animals needs to be accounted for (Anderson, 2001).

Existing methods for estimating animal density often require additional information that is often unavailable. For example, capture-mark-recapture methods (Karanth, 1995; Trolle *et al.*, 2007; Borchers *et al.*, 2014) require recognition of individuals, and distance methods (Harris *et al.*, 2013) require estimates of how far away individuals are from the sensor (Barlow & Taylor, 2005; Marques *et al.*, 2011). When individuals cannot be told apart, an extension of occupancy modelling can be used to estimate absolute abundance (Royle & Nichols, 2003). However, as the model is originally formulated to estimate occupancy, count information is simplified to presence-absence data. Assumptions about the distribution of individuals (e.g. a poisson distribution) must also be made (Royle & Nichols, 2003) which may be a poor assumption for nonrandomly distributed species. Furthermore repeat, independent surveys must be performed and the definition of a site can be difficult, especially for wide-ranging species (MacKenzie & Royle, 2005).

More recently, the development of the random encounter model (REM), a modification of an ideal gas model (Yapp, 1956; Hutchinson & Waser, 2007), has enabled

101 animal densities to be estimated from unmarked individuals of a known speed,
 102 and with known sensor detection parameters (Rowcliffe *et al.*, 2008). The REM
 103 method has been successfully applied to estimate animal densities from camera
 104 trap surveys (Manzo *et al.*, 2012; Zero *et al.*, 2013). However, extending the REM
 105 method to other types of sensors (e.g., acoustic detectors) is more problematic,
 106 because the original derivation assumes a relatively narrow sensor width (up to
 107 $\pi/2$ radians) and that the animal is equally detectable irrespective of its heading
 108 (Rowcliffe *et al.*, 2008).

109 Whilst these restrictions are not problematic for most camera trap makes (e.g.,
 110 Reconyx, Cuddeback), the REM cannot be used to estimate densities from cam-
 111 era traps with a wider sensor width (e.g. canopy monitoring with fish eye lenses,
 112 Brusa & Bunker (2014)). Additionally, the REM method is not useful in estimating
 113 densities from acoustic survey data as detector angles are often wider than $\pi/2$
 114 radians. Acoustic detectors are designed for a range of diverse tasks and envi-
 115 ronments (Kessel *et al.*, 2014), which naturally leads to a wide range of sensor de-
 116 tection widths and detection distances. In addition to this, calls emitted by many
 117 animals are directional (Blumstein *et al.*, 2011), breaking the assumption of the
 118 REM method.

119 There has been a sharp rise in interest around passive acoustic detectors in re-
 120 cent years, with a 10 fold increase in publications in the decade between 2000 and
 121 2010 (Kessel *et al.*, 2014). Acoustic monitoring is being developed to study many
 122 aspects of ecology, including the interactions of animals and their environments
 123 (Blumstein *et al.*, 2011; Rogers *et al.*, 2013), the presence and relative abundances of
 124 species (Marcoux *et al.*, 2011), biodiversity of an area (Depraetere *et al.*, 2012), and
 125 monitoring population trends (Walters *et al.*, 2013).

126 Acoustic data suffers from many of the problems associated with data from
 127 camera trap surveys in that individuals are often unmarked, making capture-
 128 mark-recapture methods more difficult to use (Marques *et al.*, 2013). In some cases
 129 the distance between the animal and the sensor is known, for example when an
 130 array of sensors is deployed and the position of the animal is estimated by trian-
 131 gulation (Lewis *et al.*, 2007). In these situations distance-sampling methods can be

132 applied, a method typically used for marine mammals (Rogers *et al.*, 2013). How-
 133 ever, in many cases distance estimation is not possible, for example when single
 134 sensors are deployed, a situation typical in the majority of terrestrial acoustic sur-
 135 veys (Elphick, 2008; Buckland *et al.*, 2008). In these cases, only relative measures
 136 of local abundance can be calculated, and not absolute densities. This means that
 137 comparison of populations between species and sites is problematic without as-
 138 suming equal detectability (Hayes, 2000; Schmidt, 2003; Walters *et al.*, 2013). Equal
 139 detectability is unlikely because of differences in environmental conditions, sensor
 140 type, habitat, and species biology.

141 In this study, we create a generalised REM (gREM) as an extension to the cam-
 142 era trap model of Rowcliffe *et al.* (2008), to estimate absolute density from count
 143 data from acoustic detectors, or camera traps, where the sensor width can vary
 144 from 0 to 2π radians, and the signal given from the animal can be directional. We
 145 assessed the accuracy and precision of the gREM within a simulated environment,
 146 by varying the sensor detection widths, animal signal widths, number of captures
 147 and models of animal movement. We use the simulation results to recommend
 148 best survey practice for estimating animal densities from remote sensors.

149 METHODS

150 **Analytical Model.** The REM presented by Rowcliffe *et al.* (2008) adapts the gas
 151 model to count data collected from camera trap surveys. The REM is derived
 152 assuming a stationary sensor with a detection width less than $\pi/2$ radians. How-
 153 ever, in order to apply this approach more generally, and in particular to stationary
 154 acoustic detectors, we need both to relax the constraint on sensor detection width,
 155 and allow for animals with directional signals. Consequently, we derive the gREM
 156 for any detection width, θ , between 0 and 2π with a detection distance r giving a
 157 circular sector within which animals can be captured (the detection zone) (Fig-
 158 ure 1). Additionally, we model the animal as having an associated signal width
 159 α between 0 and 2π (Figure 1, see Appendix S1 for a list of symbols). We start
 160 deriving the gREM with the simplest situation, the gas model where $\theta = 2\pi$ and
 161 $\alpha = 2\pi$.

162 *Gas Model.* Following Yapp (1956), we derive the gas model where sensors can
 163 capture animals in any direction and animal signals are detectable from any direc-
 164 tion ($\theta = 2\pi$ and $\alpha = 2\pi$). We assume that animals are in a homogeneous environ-
 165 ment, and move in straight lines of random direction with velocity v . We allow
 166 that our stationary sensor can capture animals at a detection distance r and that if
 167 an animal moves within this detection zone they are captured with a probability
 168 of one; while outside this zone, animals are never captured.

169 In order to derive animal density, we need to consider relative velocity from the
 170 reference frame of the animals. Conceptually, this requires us to imagine that all
 171 animals are stationary and randomly distributed in space, while the sensor moves
 172 with velocity v . If we calculate the area covered by the sensor during the survey
 173 period, we can estimate the number of animals the sensor should capture. As a
 174 circle moving across a plane, the area covered by the sensor per unit time is $2rv$.
 175 The expected number of captures, z , for a survey period of t , with an animal den-
 176 sity of D is $z = 2rvtD$. To estimate the density we rearrange to get $D = z/2rvt$. Note
 177 that as z is the number of encounters, not individuals, the possibility of repeated
 178 detections of the same individual is accounted for (Hutchinson & Waser, 2007).

179 *gREM derivations for different detection and signal widths.* Different combinations of
 180 θ and α would be expected to occur (e.g., sensors have different detection widths
 181 and animals have different signal widths). For different combinations θ and α , the
 182 area covered per unit time is no longer given by $2rv$. Instead of the size of the
 183 sensor detection zone having a diameter of $2r$, the size changes with the approach
 184 angle between the sensor and the animal. The width of the area within which an
 185 animal can be detected is called the profile, p . The size of p depends on the signal
 186 width, detector width and the angle that the animal approaches the sensor. The
 187 size of the profile (averaged across all approach angles) is defined as the average
 188 profile \bar{p} . However, different combinations of θ and α need different equations to
 189 calculate \bar{p} .

190 We have identified the parameter space for the combinations of θ and α for
 191 which the derivation of the equations are the same (defined as sub-models in the

gREM) (Figure 2). For example, the gas model becomes the simplest gREM sub-model (upper right in Figure 2) and the REM from Rowcliffe *et al.* (2008) is another gREM sub-model where $\theta < \pi/2$ and $\alpha = 2\pi$. We derive one gREM sub-model SE2 as an example below, where $2\pi - \alpha/2 < \theta < 2\pi$, $0 < \alpha < \pi$ (see Appendix S2 for derivations of all gREM sub-models). Any estimate of density would require prior knowledge of animal velocity and call width v and α taken from other sources e.g. the literature (Brinkløv *et al.*, 2011; Carbone *et al.*, 2005) and sensor width and radius, θ and r which can be measured or obtained from manufacturer specifications (Holderied & Von Helversen, 2003; Adams *et al.*, 2012).

Example derivation of SE2. In order to calculate \bar{p} , we have to integrate over the focal angle, x_1 (Figure 3a). This is the angle taken from the centre line of the sensor. Other focal angles are possible (x_2, x_3, x_4) and are used in other gREM sub-models (see Appendix S2). As the size of the profile depends on the approach angle, we present the derivation across all approach angles. When the sensor is directly approaching the animal $x_1 = \pi/2$.

Starting from $x_1 = \pi/2$ until $\theta/2 + \pi/2 - \alpha/2$, the size of the profile is $2r \sin \alpha/2$ (Figure 3b). During this first interval, the size of α limits the width of the profile. When the animal reaches $x_1 = \theta/2 + \pi/2 - \alpha/2$ (Figure 3c), the size of the profile is $r \sin(\alpha/2) + r \cos(x_1 - \theta/2)$ and the size of θ and α both limit the width of the profile (Figure 3c). Finally, at $x_1 = 5\pi/2 - \theta/2 - \alpha/2$ until $x_1 = 3\pi/2$, the width of the profile is again $2r \sin \alpha/2$ (Figure 3d) and the size of α again limits the width of the profile.

The profile width p for π radians of rotation (from directly towards the sensor to directly behind the sensor) is completely characterised by the three intervals (Figure 3b–d). Average profile width \bar{p} is calculated by integrating these profiles over their appropriate intervals of x_1 and dividing by π which gives

$$\bar{p} = \frac{1}{\pi} \left(\int_{\frac{\pi}{2}}^{\frac{\pi}{2} + \frac{\theta}{2} - \frac{\alpha}{2}} 2r \sin \frac{\alpha}{2} dx_1 + \int_{\frac{\pi}{2} + \frac{\theta}{2} - \frac{\alpha}{2}}^{\frac{5\pi}{2} - \frac{\theta}{2} - \frac{\alpha}{2}} r \sin \frac{\alpha}{2} + r \cos \left(x_1 - \frac{\theta}{2} \right) dx_1 + \int_{\frac{5\pi}{2} - \frac{\theta}{2} - \frac{\alpha}{2}}^{\frac{3\pi}{2}} 2r \sin \frac{\alpha}{2} dx_1 \right) \quad \text{eqn 1}$$

$$= \frac{r}{\pi} \left(\theta \sin \frac{\alpha}{2} - \cos \frac{\alpha}{2} + \cos \left(\frac{\alpha}{2} + \theta \right) \right) \quad \text{eqn 2}$$

217 We then use this expression to calculate density

$$218 \quad D = z/vt\bar{p}. \quad \text{eqn 3}$$

219 Rather than having one equation that describes \bar{p} globally, the gREM must be
 220 split into submodels due to discontinuous changes in p as α and β change. These
 221 discontinuities can occur for a number of reasons such as a profile switching be-
 222 tween being limited by α and θ , the difference between very small profiles and
 223 profiles of size zero, and the fact that the width of a sector stops increasing once
 224 the central angle reaches π radians (i.e., a semi-circle is just as wide as a full circle).
 225 As an example, if α is small, there is an interval between Figure 3c and 3d where
 226 the ‘blind spot’ would prevent animals being detected giving $p = 0$. This would
 227 require an extra integral in our equation, as simply putting our small value of α
 228 into eqn 1 would not give us this integral of $p = 0$.

229 gREM submodel specifications were done by hand, and the integration was
 230 done using SymPy (SymPy Development Team, 2014) in Python (Appendix S3).
 231 The gREM submodels were checked by confirming that: (1) submodels adjacent
 232 in parameter space were equal at the boundary between them; (2) submodels that
 233 border $\alpha = 0$ had $p = 0$ when $\alpha = 0$; (3) average profile widths \bar{p} were between 0
 234 and $2r$ and; (4) each integral, divided by the range of angles that it was integrated
 235 over, was between 0 and $2r$. The scripts for these tests are included in Appendix
 236 S3 and the R (Team, 2014) implementation of the gREM is given in Appendix S4.

237 **Simulation Model.** We tested the accuracy and precision of the gREM by devel-
 238 oping a spatially explicit simulation of the interaction of sensors and animals using
 239 different combinations of sensor detection widths, animal signal widths, number
 240 of captures, and models of animal movement. One hundred simulations were run
 241 where each consisted of a 7.5 km by 7.5 km square with periodic boundaries. A
 242 stationary sensor of radius r , 10 m, was set up in the exact centre of each simulated
 243 study area, covering seven sensor detection widths θ , between 0 and 2π ($2/9\pi$,
 244 $4/9\pi$, $6/9\pi$, $8/9\pi$, $10/9\pi$, $14/9\pi$, and 2π). Each sensor was set to record continuously
 245 and to capture animal signals instantaneously from emission. Each simulation
 246 was populated with a density of 70 animals km^{-2} , calculated from the equation in

247 Damuth (1981) as the expected density of mammals weighing 1 g. This density
 248 therefore represents a reasonable estimate of density of individuals, given that the
 249 smallest mammal is around 2 g (Jones *et al.*, 2009). A total of 3937 individuals per
 250 simulation were created which were placed randomly at the start of the simula-
 251 tion. 11 signal widths α between 0 and π were used ($1/11\pi$, $2/11\pi$, $3/11\pi$, $4/11\pi$,
 252 $5/11\pi$, $6/11\pi$, $7/11\pi$, $8/11\pi$, $9/11\pi$, $10/11\pi$, π).

253 Each simulation lasted for N steps (14400) of duration T (15 minutes) giving a
 254 total duration of 150 days. The individuals moved within each step with a dis-
 255 tance d , with an average speed, v . The distance, d , was sampled from a normal
 256 distribution with mean distance, $\mu_d = vT$, and standard deviation, $\sigma_d = vT/10$,
 257 where the standard deviation was chosen to scale with the average distance trav-
 258 elled. An average speed, $v = 40 \text{ km day}^{-1}$, was chosen based on the largest day
 259 range of terrestrial animals (Carbone *et al.*, 2005), and represents the upper limit of
 260 realistic speeds. At the end of each step, individuals were allowed to either remain
 261 stationary for a time step (with a given probability, S), or change direction where
 262 the change in direction has a uniform distribution in the interval $[-A, A]$. This re-
 263 sulted in seven different movement models where: (1) simple movement, where S
 264 and $A = 0$; (2) stop-start movement, where (i) $S = 0.25$, $A = 0$, (ii) $S = 0.5$, $A = 0$, (iii)
 265 $S = 0.75$, $A = 0$; (3) correlated random walk movement, where (i) $S = 0$, $A = \pi/3$, (ii)
 266 $S = 0$, $A = 2\pi/3$, (iii) $S = 0$, $A = \pi$. Individuals were counted as they moved into the
 267 detection zone of the sensor per simulation.

268 We calculated the estimated animal density from the gREM by summing the
 269 number of captures per simulation and inputting these values into the correct
 270 gREM submodel. The accuracy of the gREM was determined by comparing the
 271 true simulation density with the estimated density. Precision of the gREM was de-
 272 termined by the standard deviation of estimated densities. We used this method to
 273 compare the accuracy and precision of all the gREM submodels. As these submod-
 274 els are derived for different combinations of α and θ , the accuracy and precision of
 275 the submodels was used to determine the impact of different values of α and θ .

276 The influence of the number of captures and animal movement models on ac-
 277 curacy and precision was investigated using four different gREM submodels rep-
 278 resentative of the range α and θ values (submodels NW1, SW1, NE1, and SE3,

Figure 2). From a random starting point we ran the simulation until a range of different capture numbers were recorded (from 10 to 100 captures), recorded the length of time this took, and estimated the animal density for each of the four submodels. These estimated densities were compared to the true density to assess the impact on the accuracy and precision of the gREM. We calculated the coefficient of variation in order to compare the precision of the density estimates from simulations with different expected numbers of captures. The gREM also assumes that individuals move continuously with straight-line movement (simple movement model) and we therefore assessed the impact of breaking the gREM assumptions. We used the four submodels to compare the accuracy and precision of a simple movement model, stop-start movement models (using different average amounts of time spent stationary), and random walk movement models. As the parameters (α , β , r and v) are likely to be measured with error, we compared true simulation densities to densities estimated with parameters with errors of 0%, $\pm 5\%$ and $\pm 10\%$.

RESULTS

Analytical model. The equation for \bar{p} has been newly derived for each submodel in the gREM, except for the gas model and REM which have been calculated previously. However, many models, although derived separately, have the same expression for \bar{p} . Figure 4 shows the expression for \bar{p} in each case. The general equation for density, eqn 3, is used with the correct value of \bar{p} substituted. Although more thorough checks are performed in Appendix S3, it can be seen that all adjacent expressions in Figure 4 are equal when expressions for the boundaries between them are substituted in.

Simulation model.

gREM submodels. All gREM submodels showed a high accuracy, i.e., the median difference between the estimated and true values was less than 2% across all models (Figure 5). However, the precision of the submodels do vary, where the gas model is the most precise and the SW7 sub model the least precise, having the smallest and the largest interquartile range, respectively (Figure 5). The standard deviation of the error between the estimated and true densities is strongly related

to both the sensor and signal widths (Appendix S5), such that larger widths have lower standard deviations (greater precision) due to the increased capture rate of these models.

Number of captures. Within the four gREM submodels tested (NW1, SW1, SE3, NE1), the accuracy was not strongly affected by the number of captures. The median difference between the estimated and true values was less than 15% across all capture rates (Figure 6). However, the precision was dependent on the number of captures across all four of the gREM submodels, where precision increases as number of captures increases, as would be expected for any statistical estimate (Figure 6). For all gREM submodels, the the coefficient of variation falls to 10% at 100 captures.

Movement models. Within the four gREM submodels tested (NW1, SW1, SE3, NE1), neither the accuracy or precision was affected by the average amount of time spent stationary. The median difference between the estimated and true values was less than 2% for each category of stationary time (0, 0.25, 0.5 and 0.75) (Figure 7a). Altering the maximum change in direction in each step (0, $\pi/3$, $2\pi/3$, and π) did not affect the accuracy or precision of the four gREM submodels (Figure 7b).

Impact of parameter error. The percentage error in the density estimates across all parameters and gREM submodels shows a similar response for under and over estimated parameters, suggesting the accuracy is reasonable with respect to parameter error (Appendix S6). The impact of parameter error on the precision of the density estimate varies across and gREM submodels and parameters, where α shows the largest variation including the largest values. However, in all cases the density estimate percentage error is not more than 5% greater than the error in the parameter estimate (Appendix S6).

DISCUSSION

Analytical model. We have developed the gREM such that it can be used to estimate density from acoustic sensors and camera traps. This has entailed a generalisation of the gas model and the REM in Rowcliffe *et al.* (2008) to be applicable to any combination of sensor width θ and signal directionality α . We emphasise

that the approach is robust to multiple detections of the same individual within a survey and does not require cases of multiple capture to be removed or recorded. We have used simulations to show, as a proof of principle, that these models are accurate and precise. The precision of the gREM was found to be dependent on the number of captures which in turn depends on the width of the sensor and the signal.

There are a number of possible extensions to the gREM which could be developed in the future. The original gas model was formulated for the case where both subjects, either animal and sensor, or animal and animal, are moving (Hutchinson & Waser, 2007). Indeed any of the models with animals that are equally detectable in all directions ($\alpha = 2\pi$) can be trivially expanded by replacing animal speed v with $v + v_s$ where v_s is the speed of the sensor. However, when the animal has a directional call, as seen in both terrestrial and aquatic environments (Lammers & Au, 2003; Blumstein *et al.*, 2011), the extension becomes less simple. The approach would be to calculate again the mean profile width. However, for each angle of approach, one would have to average the profile width for an animal facing in any direction (i.e., not necessarily moving towards the sensor) weighted by the relative velocity of that direction. There are a number of situations where a moving detector and animal could occur, e.g. an acoustic detector towed from a boat when studying porpoises (Kimura *et al.*, 2014) or surveying echolocating bats from a moving car (Ahlen & Baagøe, 1999; Jones *et al.*, 2013).

Interesting but unstudied problems impacting the gREM are firstly, edge effects caused by sensor trigger delays (the delay between sensing an animal and attempting to record the encounter) (Rovero *et al.*, 2013), and secondly, sensors which repeatedly turn on and off during sampling (Jones *et al.*, 2013). The second problem is particularly relevant to acoustic detectors which record ultrasound by time expansion. Here ultrasound is recorded for a set time period and then slowed down and played back, rendering the sensor 'deaf' periodically during sampling. Both of these problems may cause biases in the gREM, as animals can move through the detection zone without being detected. As the gREM assumes constant surveillance, the error created by switching the sensor on and off quickly will become more important if the sensor is only on for short periods of time. For example, if

371 it takes longer for the recording device to be switched on than the length of some
 372 animal calls, then there could be a systematic underestimation of density. We rec-
 373 ommend that the gREM is applied to constantly sampled data, and the impacts of
 374 breaking these assumptions on the gREM should be further explored.

375 **Accuracy, Precision and Recommendations for Best Practice.** Based on our sim-
 376 ulations, we believe that the gREM has the potential to produce accurate estimates
 377 for many different species, using either camera traps or acoustic detectors. How-
 378 ever, the precision of the gREM differed between submodels. For example, when
 379 the sensor and signal width were small, the precision of the model was reduced.
 380 Therefore when choosing a sensor for use in a gREM study, the sensor detection
 381 width should be maximised. If the study species has a narrow signal direction-
 382 ality, other aspects of the study protocol, such as length of the survey, should be
 383 used to compensate.

384 The precision of the gREM is greatly affected by the number of captures. The
 385 coefficient of variation falls dramatically between 10 and 60 captures and then
 386 after this continues to slowly reduce. At 100 captures the submodels reach 10%
 387 coefficient of variation, considered to a very good level of precision (Thomas &
 388 Marques, 2012). Many current studies do not reach this level of precision, with
 389 most studies reporting coefficient of variations greater than the 10% level (O'Brien
 390 *et al.*, 2003; Proctor *et al.*, 2010; Foster & Harmsen, 2012). The length of surveys
 391 in the field will need to be adjusted so that enough data can be collected to reach
 392 this precision level. Populations of fast moving animals or populations with high
 393 densities will require less survey effort than those species that are slow moving or
 394 have populations with low densities.

395 The gREM was both accurate and precise for all the movement models we
 396 tested (stop-start movement and correlated random walks). The precision of the
 397 gREM may be affected by the interaction between the movement model and the
 398 size of the detection radius. We have studied a relatively long step length com-
 399 pared to the size of the detection radius, and therefore the chance of catching the
 400 same animal multiple times within a short space of time was reduced and there is
 401 little effect on the precision of the model (Figure 7b). However, if the ratio of step

length to detection radius was smaller, then this may decrease the precision of the model (but should not decrease its accuracy).

We found that the sensitivity of the gREM to inaccurate parameter estimates was both predictable and reasonable (Appendix S6), although this varies between different parameters and gREM submodels. Care should be taken while estimating these parameters when analysing both acoustic and camera trap data, however acoustic data poses particular problems. For acoustic surveys, estimates of r (detection distance) can be measured directly or calculated using sound attenuation models (e.g. (Holderied & Von Helversen, 2003)), while the sensor angle is often easily measured (Adams *et al.*, 2012) or in the manufacturer’s specifications. When estimating animal movement speed v , only the speed of movement during the survey period should be used. The signal width is the most sensitive parameter to inaccurate estimates (Appendix S6) and is also the most difficult to measure. While this parameter is typically assumed to be 2π for camera trap surveys, fewer estimates exist for acoustic signal widths. Although signal width has been measured for echolocating bats using arrays of microphones (Brinklöv *et al.*, 2011), more work should be done on obtaining estimates for a range of acoustically surveyed species.

Limitations. Although the REM has been found to be effective in field tests Rowcliffe *et al.* (2008); Zero *et al.* (2013), the gREM requires further validation by both field tests and simulations. For example capture-mark-recapture methods could be used alongside the gREM to test the accuracy under field conditions Rowcliffe *et al.* (2008). While we found no effect of movement on the accuracy or precision of the gREM, the movement models we have used in our simulations to validate the gREM are still simple representations of true animal movement. Animal movement may be highly nonlinear and often dependent on multiple factors such as behavioural state and existence of home ranges (Smouse *et al.*, 2010), therefore testing the gREM against real animal data, or further simulations with more complex movement models would be beneficial.

The assumptions of our simulations may require further consideration for example we have assumed an equal density across the study area. However in a

field environment the situation may be more complex, with additional variation coming from local changes in density between sensor sites. Though theoretically unequal densities should not affect accuracy (Hutchinson & Waser, 2007), it will affect precision and further simulations should be used to quantify this effect. Additionally, we allowed the sensor to be stationary and continuously detecting, negating the triggering, and non-continuous recording issues that could exist with some sensors and reduce precision or accuracy. Finally, in the simulation animals moved at the equivalent of the largest day range of terrestrial animals (Carbone *et al.*, 2005). Slower speed values should not alter the accuracy of the gREM, but precision would be affected since slower speeds produce fewer records.

Detection probability is a major focus for methods estimating density. The gREM does not fit a statistical model to estimate detection probability as occupancy models and distance sampling do (Royle & Nichols, 2003; Barlow & Taylor, 2005; Marques *et al.*, 2011). Instead it explicitly models the process, with animals only being detected if they approach the sensor from a suitable direction. More detailed models of this process could include the regularity of acoustic calls or other details.

Implications for ecology and conservation. The gREM is suitable for any species that would be consistently recorded within range of a detector, such as echolocating bats (Kunz *et al.*, 2009), songbirds (Buckland & Handel, 2006), whales (Marques *et al.*, 2009) or forest primates (Hassel-Finnegan *et al.*, 2008). With increasing technological capabilities, this list of species is likely to increase dramatically.

The gREM will aid researchers in studying species with non-invasive methods such as remote sensors which makes it suitable for large, continuous monitoring projects with limited human resources (Kelly *et al.*, 2012) and also makes them suitable for species that are sensitive to human contact or species that are difficult or dangerous to catch (Thomas & Marques, 2012).

Many of these species are critically endangered and monitoring their populations is of conservation interest. For example, density estimation for the threatened Francisana dolphin (*Pontoporia blainvillei*) (Crespo *et al.*, 2010). In addition,

using gREM it may be easier than other methods to measure the density of animals which may be useful in quantifying ecosystem services, such as songbirds with a known positive influence on pest control (Jirinec *et al.*, 2011).

ACKNOWLEDGMENTS

We thank Hilde Wilkinson-Herbot, Chris Carbone, Francois Balloux, Andrew Cunningham, Steve Hailes, Richard Glennie and an anonymous referee for comments on previous versions of the manuscript. This study was funded through CoMPLEX PhD studentships at University College London supported by BBSRC and EPSRC (EAM and TCDL); The Darwin Initiative (Awards 15003, 161333, EI-DPR075 to KEJ), and The Leverhulme Trust (Philip Leverhulme Prize for KEJ).

REFERENCES

- Acevedo, M.A. & Villanueva-Rivera, L.J. (2006) Using automated digital recording systems as effective tools for the monitoring of birds and amphibians. *Wildlife Society Bulletin*, **34**, 211–214.
- Adams, A., Jantzen, M., Hamilton, R. & Fenton, M. (2012) Do you hear what I hear? Implications of detector selection for acoustic monitoring of bats. *Methods in Ecology and Evolution*.
- Ahlen, I. & Baagøe, H.J. (1999) Use of ultrasound detectors for bat studies in Europe: experiences from field identification, surveys, and monitoring. *Acta Chiropterologica*, **1**, 137–150.
- Anderson, D.R. (2001) The need to get the basics right in wildlife field studies. *Wildlife Society Bulletin*, **29**, 1294–1297.
- Barlow, J. & Taylor, B. (2005) Estimates of sperm whale abundance in the north-eastern temperate pacific from a combined acoustic and visual survey. *Marine Mammal Science*, **21**, 429–445.
- Blumstein, D.T., Mennill, D.J., Clemins, P., Girod, L., Yao, K., Patricelli, G., Deppe, J.L., Krakauer, A.H., Clark, C., Cortopassi, K.A. *et al.* (2011) Acoustic monitoring in terrestrial environments using microphone arrays: applications, technological considerations and prospectus. *Journal of Applied Ecology*, **48**, 758–767.

- 492 Borchers, D., Distiller, G., Foster, R., Harmsen, B. & Milazzo, L. (2014) Continuous-
493 time spatially explicit capture–recapture models, with an application to a jaguar
494 camera-trap survey. *Methods in Ecology and Evolution*, **5**, 656–665.
- 495 Brinkløv, S., Jakobsen, L., Ratcliffe, J., Kalko, E. & Surlykke, A. (2011) Echoloca-
496 tion call intensity and directionality in flying short-tailed fruit bats, *Carollia per-*
497 *spicillata* (phyllostomidae). *The Journal of the Acoustical Society of America*, **129**,
498 427–435.
- 499 Brusa, A. & Bunker, D.E. (2014) Increasing the precision of canopy closure es-
500 timates from hemispherical photography: Blue channel analysis and under-
501 exposure. *Agricultural and Forest Meteorology*, **195**, 102–107.
- 502 Buckland, S.T. & Handel, C. (2006) Point-transect surveys for songbirds: robust
503 methodologies. *The Auk*, **123**, 345–357.
- 504 Buckland, S.T., Marsden, S.J. & Green, R.E. (2008) Estimating bird abundance:
505 making methods work. *Bird Conservation International*, **18**, S91–S108.
- 506 Carbone, C., Cowlshaw, G., Isaac, N.J. & Rowcliffe, J.M. (2005) How far do ani-
507 mals go? Determinants of day range in mammals. *The American Naturalist*, **165**,
508 290–297.
- 509 Crespo, E.A., Pedraza, S.N., Grandi, M.F., Dans, S.L. & Garaffo, G.V. (2010) Abun-
510 dance and distribution of endangered Franciscana dolphins in Argentine waters
511 and conservation implications. *Marine Mammal Science*, **26**, 17–35.
- 512 Damuth, J. (1981) Population density and body size in mammals. *Nature*, **290**,
513 699–700.
- 514 Depaetere, M., Pavoine, S., Jiguet, F., Gasc, A., Duvail, S. & Sueur, J. (2012) Mon-
515 itoring animal diversity using acoustic indices: implementation in a temperate
516 woodland. *Ecological Indicators*, **13**, 46–54.
- 517 Elphick, C.S. (2008) How you count counts: the importance of methods research
518 in applied ecology. *Journal of Applied Ecology*, **45**, 1313–1320.
- 519 Everatt, K.T., Andresen, L. & Somers, M.J. (2014) Trophic scaling and occupancy
520 analysis reveals a lion population limited by top-down anthropogenic pressure
521 in the Limpopo National Park, Mozambique. *PloS one*, **9**, e99389.
- 522 Foster, R.J. & Harmsen, B.J. (2012) A critique of density estimation from camera-
523 trap data. *The Journal of Wildlife Management*, **76**, 224–236.

- 524 Harris, D., Matias, L., Thomas, L., Harwood, J. & Geissler, W.H. (2013) Applying
525 distance sampling to fin whale calls recorded by single seismic instruments in
526 the northeast Atlantic. *The Journal of the Acoustical Society of America*, **134**, 3522–
527 3535.
- 528 Hassel-Finnegan, H.M., Borries, C., Larney, E., Umponjan, M. & Koenig, A. (2008)
529 How reliable are density estimates for diurnal primates? *International Journal of*
530 *Primateology*, **29**, 1175–1187.
- 531 Hayes, J.P. (2000) Assumptions and practical considerations in the design and in-
532 terpretation of echolocation-monitoring studies. *Acta Chiropterologica*, **2**, 225–
533 236.
- 534 Holderied, M. & Von Helversen, O. (2003) Echolocation range and wingbeat pe-
535 riod match in aerial-hawking bats. *Proc R Soc B*, **270**, 2293–2299.
- 536 Hutchinson, J.M.C. & Waser, P.M. (2007) Use, misuse and extensions of “ideal gas”
537 models of animal encounter. *Biological Reviews of the Cambridge Philosophical So-*
538 *ciet*y, **82**, 335–359.
- 539 Jirinec, V., Campos, B.R. & Johnson, M.D. (2011) Roosting behaviour of a migratory
540 songbird on Jamaican coffee farms: landscape composition may affect delivery
541 of an ecosystem service. *Bird Conservation International*, **21**, 353–361.
- 542 Jones, K.E., Bielby, J., Cardillo, M., Fritz, S.A., O'Dell, J., Orme, C.D.L., Safi, K.,
543 Sechrest, W., Boakes, E.H., Carbone, C., Connolly, C., Cutts, M.J., Foster, J.K.,
544 Grenyer, R., Habib, M., Plaster, C.A., Price, S.A., Rigby, E.A., Rist, J., Teacher,
545 A., Bininda-Emonds, O.R.P., Gittleman, J.L., Mace, G.M., Purvis, A. & Michener,
546 W.K. (2009) PanTHERIA: a species-level database of life history, ecology, and
547 geography of extant and recently extinct mammals. *Ecology*, **90**, 2648.
- 548 Jones, K.E., Russ, J.A., Bashta, A.T., Bilhari, Z., Catto, C., Csősz, I., Gorbachev,
549 A., Győrfi, P., Hughes, A., Ivashkiv, I., Koryagina, N., Kurali, A., Langton, S.,
550 Collen, A., Margiean, G., Pandourski, I., Parsons, S., Prokofev, I., Szodoray-
551 Paradi, A., Szodoray-Paradi, F., Tilova, E., Walters, C.L., Weatherill, A. &
552 Zavarzin, O. (2013) Indicator bats program: A system for the global acoustic
553 monitoring of bats. B. Collen, N. Pettorelli, J.E.M. Baillie & S.M. Durant, eds.,
554 *Biodiversity Monitoring and Conservation*, pp. 211–247. Wiley-Blackwell.

- 555 Karanth, K. (1995) Estimating tiger (*Panthera tigris*) populations from camera-trap
556 data using capture–recapture models. *Biological Conservation*, **71**, 333–338.
- 557 Kelly, M.J., Betsch, J., Wultsch, C., Mesa, B. & Mills, L.S. (2012) Noninvasive sam-
558 pling for carnivores. L. Boitani & R. Powell, eds., *Carnivore ecology and conserva-
559 tion: a handbook of techniques*, pp. 47–69. Oxford University Press, New York.
- 560 Kessel, S., Cooke, S., Heupel, M., Hussey, N., Simpfendorfer, C., Vagle, S. & Fisk, A.
561 (2014) A review of detection range testing in aquatic passive acoustic telemetry
562 studies. *Reviews in Fish Biology and Fisheries*, **24**, 199–218.
- 563 Kimura, S., Akamatsu, T., Dong, L., Wang, K., Wang, D., Shibata, Y. & Arai, N.
564 (2014) Acoustic capture-recapture method for towed acoustic surveys of echolo-
565 cating porpoises. *The Journal of the Acoustical Society of America*, **135**, 3364–3370.
- 566 Kunz, T.H., Betke, M., Hristov, N.I. & Vonhof, M. (2009) Methods for assessing
567 colony size, population size, and relative abundance of bats. T. Kunz & S. Par-
568 sons, eds., *Ecological and behavioral methods for the study of bats*, pp. 133–157. Johns
569 Hopkins University Press, Baltimore, Maryland, 2nd edition.
- 570 Lammers, M.O. & Au, W.W. (2003) Directionality in the whistles of Hawaiian spin-
571 ner dolphins (*Stenella longirostris*): A signal feature to cue direction of move-
572 ment? *Marine Mammal Science*, **19**, 249–264.
- 573 Lewis, T., Gillespie, D., Lacey, C., Matthews, J., Danbolt, M., Leaper, R.,
574 McLanaghan, R. & Moscrop, A. (2007) Sperm whale abundance estimates from
575 acoustic surveys of the Ionian Sea and Straits of Sicily in 2003. *Journal of the
576 Marine Biological Association of the United Kingdom*, **87**, 353–357.
- 577 MacKenzie, D.I. & Royle, J.A. (2005) Designing occupancy studies: general advice
578 and allocating survey effort. *Journal of Applied Ecology*, **42**, 1105–1114.
- 579 Manzo, E., Bartolommei, P., Rowcliffe, J.M. & Cozzolino, R. (2012) Estimation of
580 population density of European pine marten in central Italy using camera trap-
581 ping. *Acta Theriologica*, **57**, 165–172.
- 582 Marcoux, M., Auger-Méthé, M., Chmelnitsky, E.G., Ferguson, S.H. & Humphries,
583 M.M. (2011) Local passive acoustic monitoring of narwhal presence in the Cana-
584 dian Arctic: a pilot project. *Arctic*, **64**, 307–316.
- 585 Marques, T.A., Munger, L., Thomas, L., Wiggins, S. & Hildebrand, J.A. (2011) Es-
586 timating North Pacific right whale (*Eubalaena japonica*) density using passive

- 587 acoustic cue counting. *Endangered Species Research*, **13**, 163–172.
- 588 Marques, T.A., Thomas, L., Martin, S.W., Mellinger, D.K., Ward, J.A., Moretti, D.J.,
589 Harris, D. & Tyack, P.L. (2013) Estimating animal population density using pas-
590 sive acoustics. *Biological Reviews*, **88**, 287–309.
- 591 Marques, T.A., Thomas, L., Ward, J., DiMarzio, N. & Tyack, P.L. (2009) Estimating
592 cetacean population density using fixed passive acoustic sensors: An example
593 with Blainville’s beaked whales. *The Journal of the Acoustical Society of America*,
594 **125**, 1982–1994.
- 595 O’Brien, T.G., Kinnaird, M.F. & Wibisono, H.T. (2003) Crouching tigers, hidden
596 prey: Sumatran tiger and prey populations in a tropical forest landscape. *Animal*
597 *Conservation*, **6**, 131–139.
- 598 Proctor, M., McLellan, B., Boulanger, J., Apps, C., Stenhouse, G., Paetkau, D. &
599 Mowat, G. (2010) Ecological investigations of grizzly bears in Canada using
600 DNA from hair, 1995–2005: a review of methods and progress. *Ursus*, **21**, 169–
601 188.
- 602 Purvis, A., Gittleman, J.L., Cowlshaw, G. & Mace, G.M. (2000) Predicting extinc-
603 tion risk in declining species. *Proceedings of the Royal Society of London Series B:*
604 *Biological Sciences*, **267**, 1947–1952.
- 605 Rogers, T.L., Ciaglia, M.B., Klinck, H. & Southwell, C. (2013) Density can be mis-
606 leading for low-density species: benefits of passive acoustic monitoring. *Public*
607 *Library of Science One*, **8**, e52542.
- 608 Rovero, F., Zimmermann, F., Berzi, D. & Meek, P. (2013) “Which camera trap type
609 and how many do I need?” a review of camera features and study designs for a
610 range of wildlife research applications. *Hystrix*, **24**, 148–156.
- 611 Rowcliffe, J.M. & Carbone, C. (2008) Surveys using camera traps: are we looking
612 to a brighter future? *Animal Conservation*, **11**, 185–186.
- 613 Rowcliffe, J., Field, J., Turvey, S. & Carbone, C. (2008) Estimating animal density
614 using camera traps without the need for individual recognition. *Journal of Ap-*
615 *plied Ecology*, **45**, 1228–1236.
- 616 Royle, J.A. & Nichols, J.D. (2003) Estimating abundance from repeated presence-
617 absence data or point counts. *Ecology*, **84**, 777–790.

- Schmidt, B.R. (2003) Count data, detection probabilities, and the demography, dynamics, distribution, and decline of amphibians. *Comptes Rendus Biologies*, **326**, 119–124.
- Smouse, P.E., Focardi, S., Moorcroft, P.R., Kie, J.G., Forester, J.D. & Morales, J.M. (2010) Stochastic modelling of animal movement. *Philosophical Transactions of the Royal Society B: Biological Sciences*, **365**, 2201–2211.
- SymPy Development Team (2014) *SymPy: Python library for symbolic mathematics*.
- Team, R.C. (2014) *R: A Language and Environment for Statistical Computing*. R Foundation for Statistical Computing, Vienna, Austria.
- Thomas, L. & Marques, T.A. (2012) Passive acoustic monitoring for estimating animal density. *Acoustics Today*, **8**, 35–44.
- Trolle, M., Noss, A.J., Lima, E.D.S. & Dalponte, J.C. (2007) Camera-trap studies of maned wolf density in the Cerrado and the Pantanal of Brazil. *Biodiversity and Conservation*, **16**, 1197–1204.
- Walters, C.L., Collen, A., Lucas, T., Mroz, K., Sayer, C.A. & Jones, K.E. (2013) Challenges of using bioacoustics to globally monitor bats. R.A. Adams & S.C. Pedersen, eds., *Bat Evolution, Ecology, and Conservation*, pp. 479–499. Springer.
- Walters, C.L., Freeman, R., Collen, A., Dietz, C., Brock Fenton, M., Jones, G., Obrist, M.K., Puechmaille, S.J., Sattler, T., Siemers, B.M. *et al.* (2012) A continental-scale tool for acoustic identification of European bats. *Journal of Applied Ecology*, **49**, 1064–1074.
- Wright, S.J. & Hubbell, S.P. (1983) Stochastic extinction and reserve size: a focal species approach. *Oikos*, pp. 466–476.
- Yapp, W. (1956) The theory of line transects. *Bird Study*, **3**, 93–104.
- Zero, V.H., Sundaresan, S.R., O'Brien, T.G. & Kinnaird, M.F. (2013) Monitoring an endangered savannah ungulate, Grevy's zebra (*Equus grevyi*): choosing a method for estimating population densities. *Oryx*, **47**, 410–419.

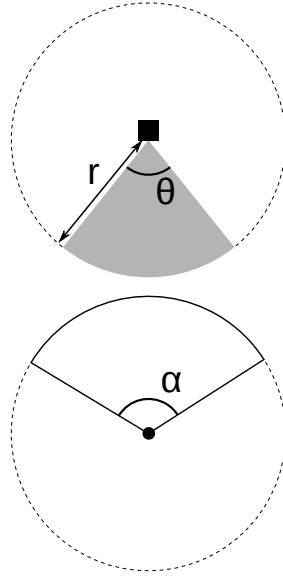


Figure 1. Representation of sensor detection width and animal signal width. The filled square and circle represent a sensor and an animal, respectively; θ , sensor detection width (radians); r , sensor detection distance; dark grey shaded area, sensor detection zone; α , animal signal width (radians). Dashed lines around the filled square and circle represents the maximum extent of θ and α , respectively.

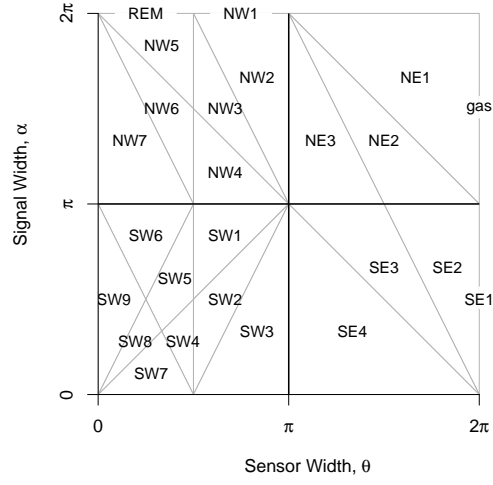


Figure 2. Locations where derivation of the average profile \bar{p} is the same for different combinations of sensor detection and animal signal widths. Symbols within each polygon refer to each gREM submodel named after their compass point, except for Gas and REM which highlight the position of these previously derived models within the gREM. Symbols on the edge of the plot are for submodels where $\alpha, \theta = 2\pi$

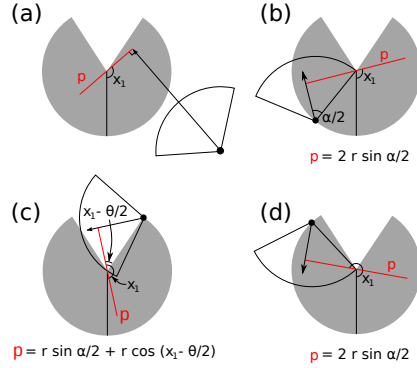


Figure 3. An overview of the derivation of the average profile \bar{p} for the gREM submodel SE2, where (a) shows the location of the profile p (the line an animal must pass through in order to be captured) in red and the focal angle, x_1 , for an animal (filled circle), its signal (unfilled sector), and direction of movement (shown as an arrow). The detection zone of the sensor is shown as a filled grey sector with a detection distance of r . The vertical black line within the circle shows the direction the sensor is facing. The derivation of p changes as the animal approaches the sensor from different directions (shown in b-d), where (b) is the derivation of p when x_1 is in the interval $[\frac{\pi}{2}, \frac{\pi}{2} + \frac{\theta}{2} - \frac{\alpha}{2}]$, (c) p when x_1 is in the interval $[\frac{\pi}{2} + \frac{\theta}{2} - \frac{\alpha}{2}, \frac{5\pi}{2} - \frac{\theta}{2} - \frac{\alpha}{2}]$ and (d) p when x_1 is in the interval $[\frac{5\pi}{2} - \frac{\theta}{2} - \frac{\alpha}{2}, \frac{3\pi}{2}]$, where θ , sensor detection width; α , animal signal width. The resultant equation for p is shown beneath b-d. The average profile \bar{p} is the size of the profile averaged across all approach angles.

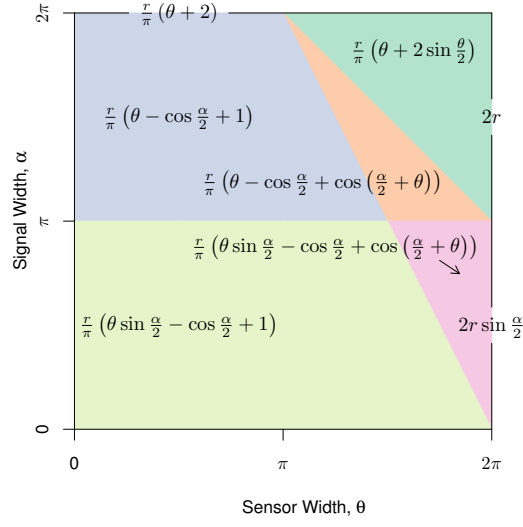


Figure 4. Expressions for the average profile width, \bar{p} , given a range of sensor and signal widths. Despite independent derivation within each block, many models result in the same expression. These are collected together and presented as one block of colour. Expressions on the edge of the plot are for submodels with $\alpha, \theta = 2\pi$.

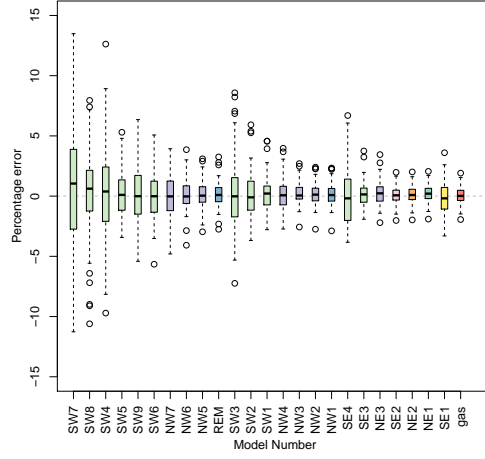


Figure 5. Simulation model results of the accuracy and precision for gREM submodels. The percentage error between estimated and true density for each gREM sub model is shown within each box plot, where the black line represents the median percentage error across all simulations, boxes represent the middle 50% of the data, whiskers represent variability outside the upper and lower quartiles with outliers plotted as individual points. Box colours correspond to the expressions for average profile width \bar{p} given in Figure 4.

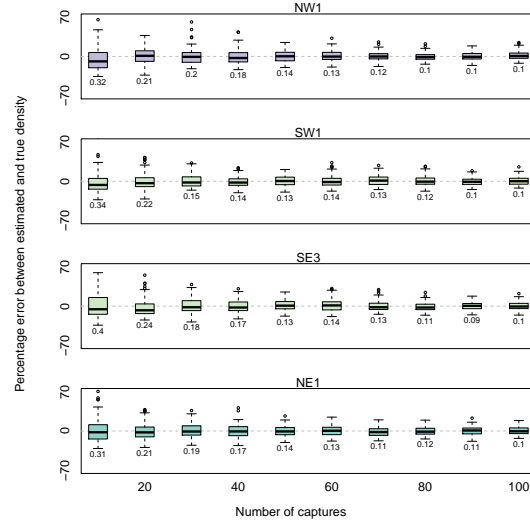


Figure 6. Simulation model results of the accuracy and precision of four gREM submodels (NW1, SW1, SE3 and NE1) given different numbers of captures. The percentage error between estimated and true density within each gREM sub model for capture rate is shown within each box plot, where the black line represents the median percentage error across all simulations, boxes represent the middle 50% of the data, whiskers represent variability outside the upper and lower quartiles with outliers plotted as individual points. Sensor and signal widths vary between submodels. The numbers beneath each plot represent the coefficient of variation. The colour of each box plot corresponds to the expressions for average profile width \bar{p} given in Figure 4.

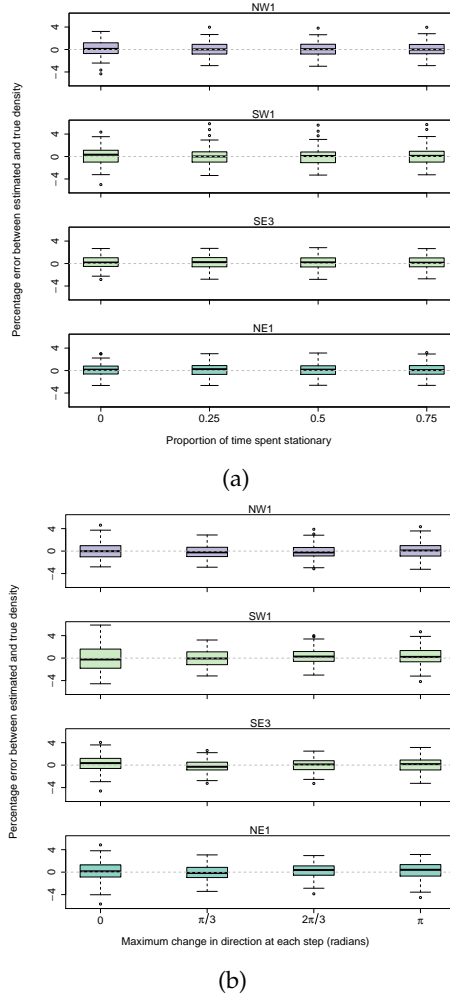


Figure 7. Simulation model results of the accuracy and precision of four gREM submodels (NW1, SW1, SE3 and NE1) given different movement models where (a) average amount of time spent stationary (stop-start movement) and (b) maximum change in direction at each step (correlated random walk model). The percentage error between estimated and true density within each gREM sub model for the different movement models is shown within each box plot, where the black line represents the median percentage error across all simulations, boxes represent the middle 50% of the data, whiskers represent variability outside the upper and lower quartiles with outliers plotted as individual points. The simple model is represented where time and maximum change in direction equals 0. The colour of each box plot corresponds to the expressions for average profile width \bar{p} given in Figure 4.